Andrzej Gradzik, Jacek Nawrocki, Grażyna Mrówka-Nowotnik, Jan Sieniawski

Laser Surfacing of Superalloy Inconel 738LC-Based Alloy Stellite 694 – Overlay Weld Imperfections

Abstract: The research involved the analysis of test results concerning the effect of laser surfacing process conditions on the characteristics of an overlay weld made of alloy Stellite 694 on the substrate of nickel superalloy Inconel 738LC as well as the determination and specification of the most common overlay weld imperfections. The overlay weld subjected to the tests was made using a Yb:YAG disc laser having a power of 1 kW and a filler metal in the form of powdered Stellite 694 cobalt alloy. The research led to the development of process conditions and the identification of major overlay weld imperfections including lacks of penetration, gas pores and microcracks in the base material. The formation of above-named imperfections could be ascribed to low laser radiation power density (< 30 kW/cm^2), the excessive overlap of consecutive tracks (> 60% of the single track width) and the insufficient gas shielding of liquid metal in the weld pool.

Keywords: laser surfacing, substrate Inconel 738LC, overlay weld Stellite 694, microstructural morphology, overlay weld imperfections

DOI: *10.17729/ebis.2017.4/3*

Introduction

Nickel superalloys are widely used in the manufacturing of elements of the hot part of aero-engines, e.g. blades of the 1st and 2nd degree of the high-pressure turbine. The above-named blades are operated in particularly harsh conditions, i.e. exposition to high temperature and oxidising gases. The wear of blades during the engine operation results from high-temperature corrosion and erosion in the stream of hot gases. Shelves of blades forming the external ring of individual turbine stages are also exposed to abrasive wear [1, 2]. For this reason, the contact surface of the above-named shelves is provided (through surfacing) with the protective layer characterised by higher resistance than that of nickel superalloys. The protective layer is usually made of cobalt alloys having the high content of carbon (0.5–2.5 % by weight), chromium (28–33 % by weight) and tungsten (4–19 % by weight) [3–5]. The layer is made using conventional gas and electric surfacing, thermal spraying as well as using technologically advanced plasma and laser-based surfacing methods. Laser welding enables the precise making of layers characterised by forecast properties, particularly on small-sized elements of complex shapes [4–8]. The laser beam used in

mgr inż. Andrzej Gradzik (MSc Eng.); mgr inż. Jacek Nawrocki (MSc Eng.); dr hab. inż. Grażyna Mrówka-Nowotnik (PhD (DSC) habilitated. Eng.), Professor at Rzeszów University of Technology; prof. dr hab. inż. Jan Sieniawski (Professor PhD (DSc) habilitated Eng.) – Rzeszów University of Technology

the surfacing process makes it possible to control the molten volume of the filler metal and base material. The filler metal, usually in the form of powder, is fed through the side nozzle or openings in the laser head nozzle. The (powdered) filler metal feeding rate is usually restricted within the range of 1 to 50 g/min [7, 8]. Laser surfacing is usually shielded by inert gas, e.g. helium or argon. The surfacing rate is connected with the travel rate of the laser head in relation to the base material and is usually restricted within the range of 100 to 1000 mm/min [7, 8, 10–12].

The laser beam-surfaced overlay weld is usually composed of its individual overlapping tracks. An important factor affecting the quality of the overlay weld is the degree of the overlapping of its subsequent tracks as it determines the presence of such imperfections as the lack of penetration or the excessive penetration of the base material. In addition, overlay welds may also contain gas pores, which can be primarily ascribed to the insufficient gas shielding during surfacing or because of the surfacing process performed at an excessively high surfacing rate [4, 6–8].

The analysis of reference publications revealed that, during welding and surfacing, casting nickel superalloys tend to develop cracks in the fusion line area, along grain boundaries or interdendritic spaces. The reason for crack formation is the partial melting of microstructural phase constituents significantly varying in terms of thermodynamic, thermal and physical properties, i.e. eutectics (γ+γ') as well as the precipitation of intermetallic phases, i.e. MC, M_6C and $M_{23}C_6$ type carbides and M3B2 borides characterised by high contents of Cr, Mo, Ti and Ta and Ti(C,N) carbonitrides present in nickel superalloy grain boundaries during welding and surfacing [2, 13–19]. The objective of the research was to identify and characterise the most common imperfections present in overlay welds made in alloy Stellite 694 on the base material of nickel superalloy Inconel 738LC. The above-named identification was necessary to increase the abrasive resistance of blade shelf contact surface in friction conditions.

Test Materials and Testing Methodology

The research involved tests of layers made using laser surfacing on the base material of nickel superalloy Inconel 738LC having the following chemical composition in % by weight: Cr – 16, Co – 8.5, Al – 4, Ti – 3.4, W – 2.3, Mo – 1.8, Ta – 1.5, Nb – 0.7, C – 0.1 and Ni – the rest. The filler metal was powdered cobalt alloy Stellite 694 (Fig. 1) having the following content in % by weight Cr – 28, W – 18.6, Ni – 5.4, V – 0.8, C – 0.85, Co – the rest and having particle diameters restricted within the range of 30 to 80 μm (Fig. 2).

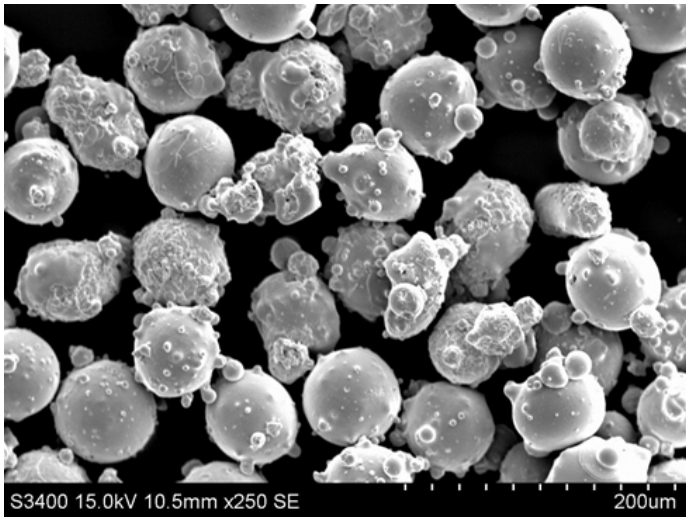

Fig. 1. Powdered cobalt alloy – Stellite 694

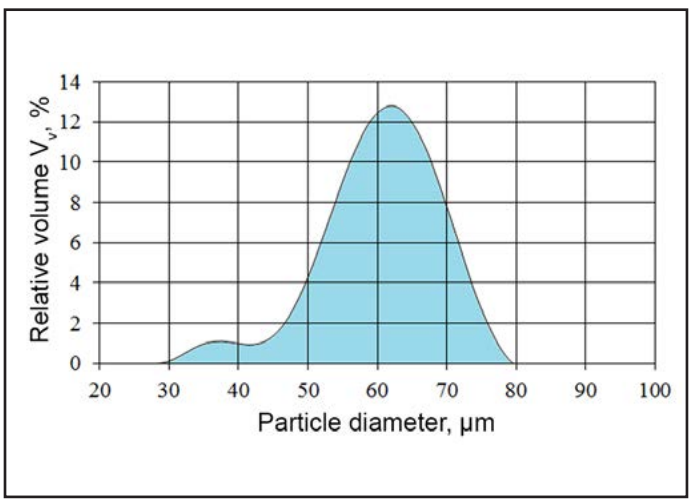

Fig. 2. Distribution of Stellite 694 particle diameter

The process of laser surfacing was performed using a TruLaser Cell 3008 device and a Yb:YAG TruDisk 1000 disc laser (TRUMPF) (Fig. 3). The carrier gas for Stellite 694 was helium, whereas the shielding gas was argon. The purity class of technical gases was N5.0.

Fig. 3. Test rig for laser surfacing (a), laser head (b)

The surfacing process involved the use of a continuous laser radiation beam having a power restricted within the range of 121 to 370 W and a diameter on the base material surface restricted within the range of 0.7 to 1.24 mm. The above-named adjustment of laser radiation beam power and of its diameter enabled the obtainment of power density of approximately 30.5 kW/cm^2. Powdered cobalt alloy (Stellite 694) was fed through three openings of the laser head nozzle. The cobalt alloy powder was fed at a rate restricted within the range of 2.8 to 5.2 g/min, the carrier gas (helium) flow rate was 5 dm3/min., whereas the shielding gas (argon) flow rate was restricted within the range of 9 to 15 dm3/min. In subsequent tracks the laser beam was moved by a distance amounting to between 40 and 60% of the single track width. The microscopic tests of the overlay weld were performed using a Nikon Epiphot 300 light microscope and a Hitachi S-3400N scanning electron microscope. The surface of metallographic specimens was etched using a reagent having the following chemical composition: HCl – 80 cm^3 + HNO_3 – 2 cm^3 + H_2O – 11 cm^3 + $FeCl_3$ – 16 g. The hardness of the overlay weld was measured using a Nexus 4303 hardness tester, the Vickers hardness test and a load of 4.9 N.

Test Results and Analysis

The macroscopic tests of the overlay weld surface revealed the presence of partially melted powder particles. Effects related to the oxidation of overlay weld surface subjected to laser surfacing were not observed.

The morphology of microstructural phase constituents identified in the microscopic tests of the overlay weld made it possible to determine the course of the solidification of subsequent overlay weld tracks (Fig. 4). The overlay weld structure was dendritic. The dendrites grew on the partially melted base material of superalloy Inconel 738LC and in previously made and partially remolten tracks of the overlay weld. The overlay weld hardness amounting to approximately 600 HV0.5 was higher than that of the base material (and amounting to approximately 400 HV 0.5) and did not change significantly across the overlay weld cross-section (Fig. 5).

The microscopic tests revealed the presence of gas pores in the overlay weld material. The pores were characterised by a spherical shape (Fig. 6) and dimensions restricted within the range of 4 to 40 μm. Most of the pores proved to have a diameter restricted within the range of 4 to 15 μm (Fig. 7). The number of gas pores

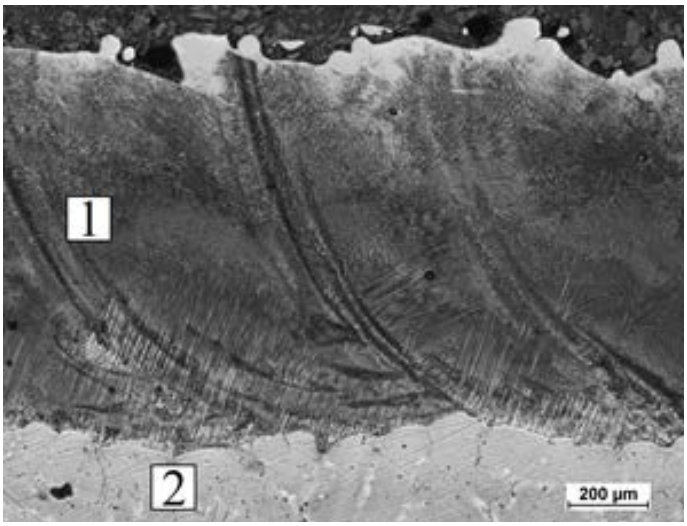

Fig. 4. Microstructure of the overlay weld made in Stellite 694 (1) on the base material of nickel superalloy Inconel 738LC (2)

in the overlay weld increased along with a decrease in the movement of the laser beam in subsequent tracks. It was also revealed that the movement of the laser beam by 60% of the single track width resulted in the excessive melting of the base material leading to the formation of the irregular surface of the fusion line and of the weld (Fig. 8a). A decrease in the laser beam movement in the subsequent track to 50% of the single track width resulted in the significant decrease of the above-named phenomenon and, at the same time, enabled the obtainment of the proper baser material penetration (Fig. 8b).

The analysis of the shape and dimensions of the weld revealed that a decrease in the laser beam movement by 40% of the single track width resulted in an increase in the overlay weld height and a decrease in its width. At the same time it was observed that the filler metal powder feeding rate > 5 g/min (Fig. 9) resulted in the lack of base material penetration.

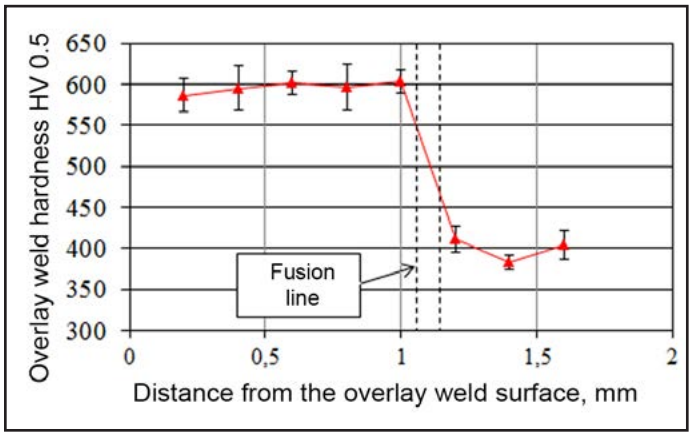

Fig. 5. Hardness distribution of the overlay weld made in Stellite 694 on the base material of nickel superalloy Inconel 738LC in the function of the distance from the surface

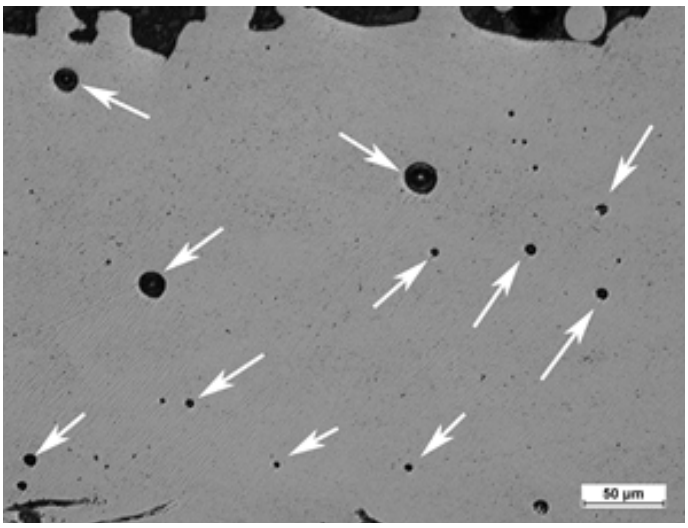

Fig. 6. Cross-section of the overlay weld made in Stellite 694 on the base material of superalloy Inconel 738LC – visible gas pores

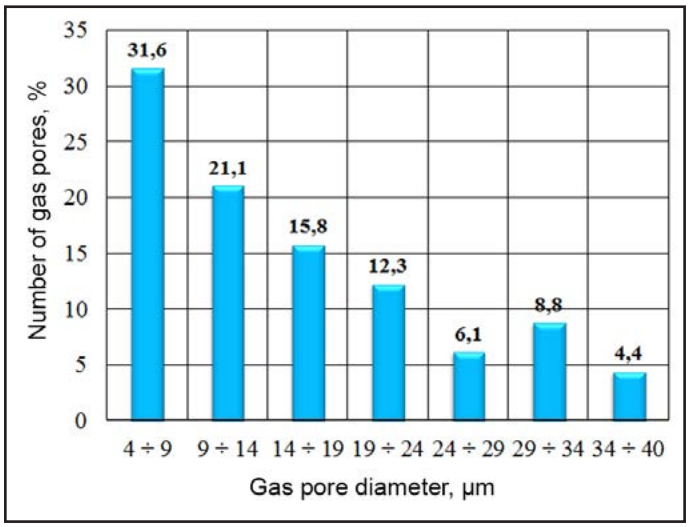

Fig. 7. Distribution of gas pore diameters in the overlay weld made in Stellite 694 on the base material of nickel superalloy Inconel 738LC

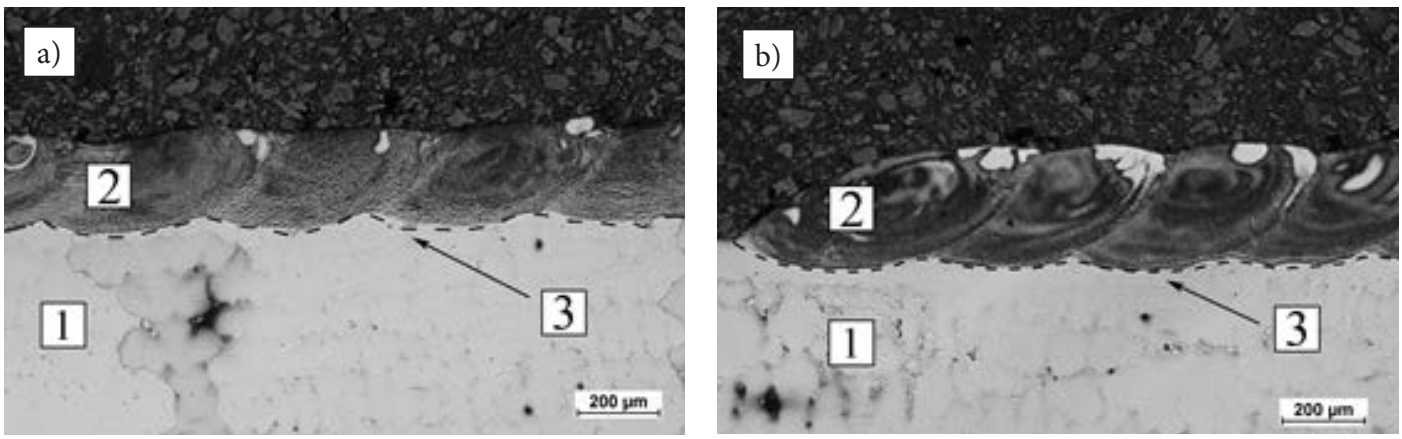

Fig. 8. Microstructural cross-section of the overlay weld made in Stellite 694 (2) on the base material of nickel superalloy Inconel 738LC (1) with the laser beam moving by: a) 40% of the single track width, b) 50% of the single track width; visible irregular fusion line (3)

The microscopic tests also revealed that microcracks in the base material formed during the surfacing process were located near the fusion line, i.e. along grain boundaries (Fig. 10). The reason for the formation of the microcracks was the presence of intermetallic phases (Ti(C,N) carbonitrides, MC, M_6C and $M_{23}C_6$ carbides as well as M_3B_2 borides characterised by significant contents of Cr, Mo, Ti and Ta) as well as the presence of eutectics (γ+γ') along the base material (Inconel 738LC) grain boundaries. The individual microstructural phase constituents of the nickel superalloy are characterised by significantly varying thermodynamic, thermal and physical properties. For this reason, the partial melting of the above-named constituents during laser surfacing triggers significant changes in internal stresses along the grain boundaries leading to the nucleation of microcracks followed by their propagation in the heat affected zone of the subsequent overlay weld track.

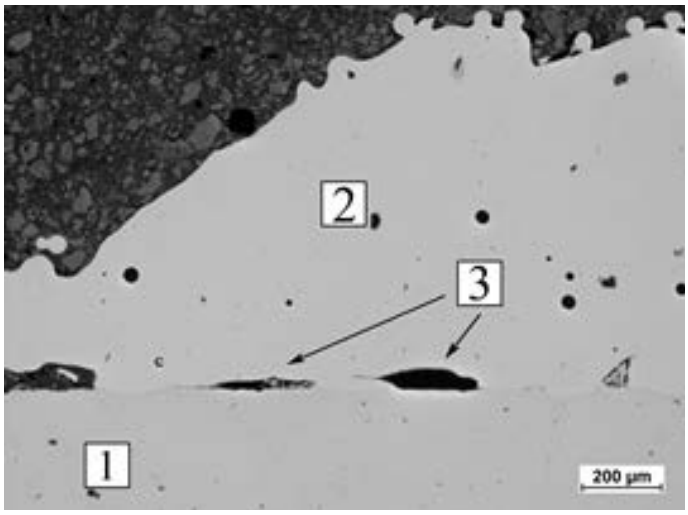

Fig. 9. Microstructure of the overlay weld made in Stellite 694 (2) on the base material of nickel superalloy 738LC (1). Laser radiation beam power of 250 W, laser beam diameter on the base material of 1.02 mm, powder feeding rate of 5.2 g/min, surfacing rate of 400 mm/min, laser beam travel in subsequent tracks: 40% of the single track width; visible lack of penetration in the base material (3)

Summary

By making many overlapping tracks, the developed conditions of laser surfacing with the filler metal, i.e. powdered cobalt alloy Stellite 694, on the base material of nickel superalloy Inconel 738LC enable the making of an overlay weld characterised by a hardness of approximately 600 HV 0,5. The overlay material structure was dendritic. The dendrites grew on the base material of superalloy Inconel 738LC and in partially remolten overlay weld tracks.

The analysis of microscopic test results revealed the presence of overlay weld imperfections in relation to most of the applied laser surfacing process conditions (gas pores, fusion line irregular surface, lack of penetration and microcracks). The gas pores tended to be spherical (< 40 µm). The reason for the formation of the gas pores lied in the insufficient gas shielding, i.e. overly low argon glow rate. It was also ascertained that the overly low overlay weld track overlapping degree (40% of the single track width) led to the melting of the significant amount of the base material and the formation of the irregular fusion line surface. In turn, the excessively high overlay weld track overlapping degree (> 60% of the single track width) resulted in the lack of the

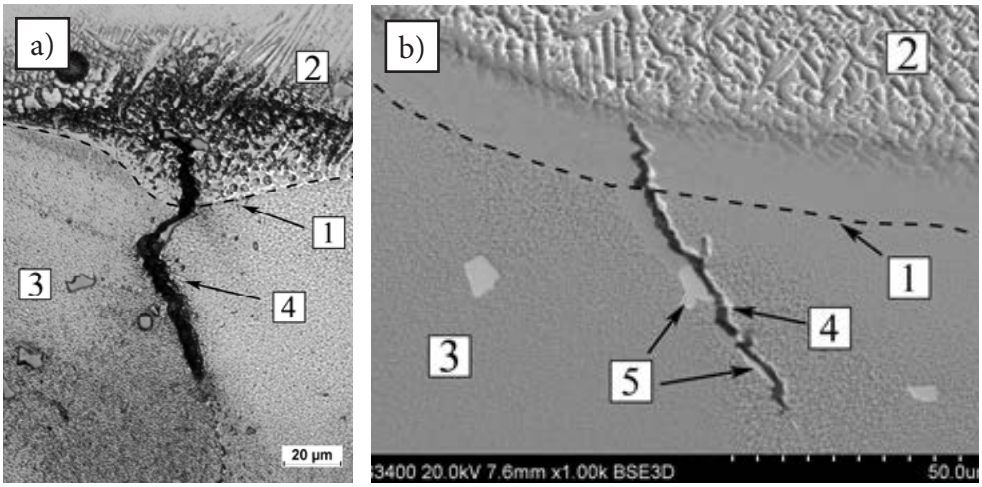

Fig. 10. Microstructure of the area near the fusion line (1) of the overlay weld made in Stellite 694 (2) on the base material of nickel superalloy Inconel 738LC (3); visible microcrack along the boundary of the base material (4) and intermetallic phase precipitates, i.e. Ti(C,N) carbonitrides (5)

melting of the base material i.e. nickel superalloy Inconel 738LC.

The microscopic test results revealed the presence of microcracks in the fusion line area. The microcracks were formed during overlay weld solidification and were usually located along the base material (Inconel 738LC) grain boundaries. The melting and solidification of the base material (Inconel 738LC) microstructure phase constituents and of the filler metal (Stellite 694), characterised by significantly varying thermodynamic properties (solid solution, intermetallic phases, i.e. MC, M_6C and $M_{23}C_6$ carbides, M_3B_2 borides and Ti(C,N) carbonitrides) triggered the generation of thermal stresses in the overlay weld and in the heat affected zone leading to the initiation of microcracks along the base material grain boundaries.

The research work was performed within programme INNOLOT, contract no. INNOLOT/I/7/NCBR/2013 "Advanced Techniques in the Manufacture of the Power Turbine Unit",co-financed by the National Centre for Research and Development.

References

[1] Sieniawski J.: *Kryteria i sposoby oceny materiałów na elementy lotniczych silników turbinowych*. Oficyna Wydawnicza Politechniki Rzeszowskiej, Rzeszów, 1995.

[2] Reed C. R.: *The superalloys: Fundamentals and applications*. Cambridge University Press, Cambridge, 2006. http://dx.doi.org/10.1017/cbo9780511541285

[3] Davis J. R.: *Asm Specialty Handbook – nickel, cobalt and their alloys*. Asm International, Ohio, 2000.

[4] Klimpel A.: *Napawanie i natryskiwanie cieplne*. Wnt, Warszawa, 2000.

[5] Burakowski T., Wierzchoń T.: *Inżynieria powierzchni metali*. Wnt, Warszawa, 1995.

[6] Klimpel A.: T*echnologie laserowe – spawanie, napawanie, stopowanie, obróbka cieplna i cięcie*. Wydawnictwo Politechniki Śląskiej, Gliwice, 2012.

[7] Gradzik A., Mrówka-Nowotnik G., Nawrocki J., Sieniawski J.: *Wpływ warunków procesu napawania laserowego na mikrostrukturę i twardość napoiny Stellite 694 na podłożu z nadstopu niklu Inconel 738LC*. Mechanik, 2016, t. 89, no. 4, pp. 276-281. http://dx.doi.org/10.17814/mechanik.2016.4.36

[8] Ion J. C.: *Laser Processing of Engineering Materials*. Elsevier, Oxford, 2005.

[9] Toyserkani E., Khajepour A., Corbin S.: *Laser Cladding*. Crc Press llc, Boca Raton, 2005.

[10] Nowotny S., Scharek S., Beyer E., Richter K. H.: *Laser beam build-up welding: precision in repair, surface cladding, and direct 3d metal deposition*. Journal of Thermal Spray Technology, 2007, vol. 16, no. 3, pp. 345-348. http://dx.doi.org/10.1007/s11666-007-9028-5

[11] Syed W. U. H., Pinkerton A. J., Li L.: *A comparative study of wire feeding and powder feeding in direct diode laser deposition for rapid prototyping*. Applied Surface Science, 2005, vol. 247, no. 1-4, pp. 268–276. http://dx.doi.org/10.1016/j.apsusc.2005.01.138

[12] Sexton L., Lavin S., Byrne G., Kennedy A.: *Laser cladding of aerospace materials*. Journal of Materials Processing Technology, 2002, vol 122, no. 1, pp. 63-68. http://dx.doi.org/10.1016/s0924-0136(01)01121-9

[13] Sidhu R. K., Ojo O. A., Chaturvedi M. C.: *Microstructural analysis of laser-beam-welded directionally solidified Inconel 738*. Metallurgical and Materials Transactions A, 2007, vol. 38, no. 4, pp. 858-870. http://dx.doi.org/10.1007/s11661-006-9063-8

[14] Lachowicz M., Dudziński W., Haimann K., Podrez-Radziszewska M.: *Microstructure transformations and cracking in the matrix of γ–γ' superalloy Inconel 713C melted with electron beam*. Materials Science and Engineering A, 2008, vol. 479,

no. 1-2, pp. 269-276.
http://dx.doi.org/10.1016/j.msea.2007.06.064
[15] Montazeri M., Malek Ghaini F., Ojo O. A.: *Heat input and the liquation cracking of laser welded IN738LC superalloy*. Welding Journal, 92 (2013) 9, pp. 258-264.
[16] Durand-Charre M.: *The microstructure of superalloys*. Gordon and Breach Science Publishers, London, 2003.
[17] El-Bagoury N., Nofal A.: *Microstructure of an experimental Ni base superalloy under various casting conditions.* Materials Science and Engineering A, 2010, vol. 527, no. 29-30, pp. 7793-7800.
http://dx.doi.org/10.1016/j.msea.2010.08.050
[18] Idowu O.A., Ojo O.A., Chaturvedi M.C.: *Microstructural Study of Transient Liquid Phase Bonded Cast Inconel 738LC Superalloy*. Metallurgical and Materials Transactions A, 2006, vol. 37, no. 9, pp. 2787-2796.
http://dx.doi.org/10.1007/bf02586111
[19] Lippold J. C.: *Welding metallurgy and weldability*. John Wiley & Sons, New Jersey. 2015.
http://dx.doi.org/10.1002/9781118960332